Compensation of Chromatic Dispersion by Modal Dispersion in MMF- and VCSEL-Based Gigabit Ethernet Transmissions

Asghar Gholami, Denis Molin, and Pierre Sillard

Abstract—**Multimode vertical-cavity surface-emitting lasers (VCSELs) with large spectral widths are widely used with multimode fibers (MMFs) in Gigabit Ethernet (GbE) systems. MMFs exhibit large chromatic dispersion values that can strongly impact the performance of these systems for high bit rates and/or long distances. Here, we show that in 10-GbE systems using VCSELs and MMFs, the chromatic dispersion can be compensated for by the modal dispersion of the MMF.**

Index Terms—**Chromatic dispersion, multimode fiber (MMF), modal dispersion, vertical-cavity surface-emitting laser (VCSEL).**

I. INTRODUCTION

IN multimode fibers (MMFs) the refractive index profile is optimized to reduce the modal dispersion in order to provide the maximum bandwidth for data transmissions.

The optimized profile is well known. It consists of a graded index part (the core) that follows a power law parameterized by the so-called α parameter, surrounded by a constant cladding

$$ n(r) = n_0 \cdot \sqrt{1 - 2\Delta \left(\frac{r}{a}\right)^\alpha} \quad \Delta = \frac{(n_0 - n_1)}{n_0} $$

where n_0, n_1, a, and r are the refractive index in the center, the refractive index in the cladding, the radius of core, and the radial coordinate $(\leq a)$, respectively.

The bandwidth of such an MMF is limited by the modal dispersion, which is minimal at α_{optimum}, but also by the chromatic dispersion that mainly depends on the material dispersion. The standardized differential mode delay (DMD) measurement provides modal dispersion cartographies, also called DMD plots, that are then postprocessed in order to derive modal dispersion parameters (DMD values, effective modal bandwidth computed (EMBc), ect.) [1]. In this letter, we focus on EMBc, which is a rough estimation of the minimal modal bandwidth that can be obtained over the authorized launching conditions.

High-speed optoelectronic modules using vertical-cavity surface-emitting lasers (VCSELs) coupled to MMFs are mainly used in typical 10-Gigabit Ethernet (10-GbE) short-distance op-
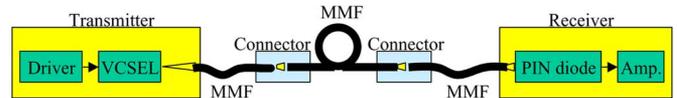
Fig. 1. Overview of the system.

tical links (see Fig. 1). Generally, they are transversally multimode and longitudinally single-mode with a discrete and large [up to 0.45-nm root mean square (rms)] spectrum in the 840- to 860-nm window.

The relatively large chromatic dispersion value of typical 50-μm MMF (~ -100 ps/nm$\cdot$km at 850 nm) limits the distance of GbE systems. It can be neglected in 300-m-long (OM3 fiber) 10-GbE systems [2], but not in 550-m-long (OM4 fiber) or in longer and/or higher bit-rate systems.

This letter focuses on how chromatic and modal dispersion interact and how they can compensate for each other when the MMF is used with a standard VCSEL. The principle of modal and chromatic dispersion interference (MCDI) will be explained, simulated, and compared to experimental results.

II. SIMULATIONS

A. Model

We have implemented a complete physical model of 10-GbE systems [3] that includes an advanced model of VCSEL [4]. This latter model computes the noise and signal carried by each VCSEL mode under a direct current modulation. The noise and signal are indeed different from one VCSEL mode to another because of carrier diffusion and spatial-hole burning phenomena, also known as mode partition noise (MPN) and mode competition, respectively. For the coupling between the VCSEL and the MMF, we compute the mode power distributions in the MMF induced by each VCSEL mode, taking into account the connectors between fibers [2], [3], [5]. The propagation of signals and noises of each VCSEL mode is then performed in the Fourier domain, knowing the group velocity and the chromatic dispersion of each fiber mode that is computed by solving the scalar wave equation at each VCSEL mode wavelength [6]. The intersymbol interference (ISI) and its interaction with MPN are thus taken into account in our model. Then, the quantum noise, dark noise, and amplifier noises coming from the receiver (photodiode and amplifiers) are added. Finally, the bit-error-rate (BER) estimation is performed taking in account ISI, transmitter and receiver noises, and time and amplitude jitters [3]. The EMBc is simulated separately using our fiber model.
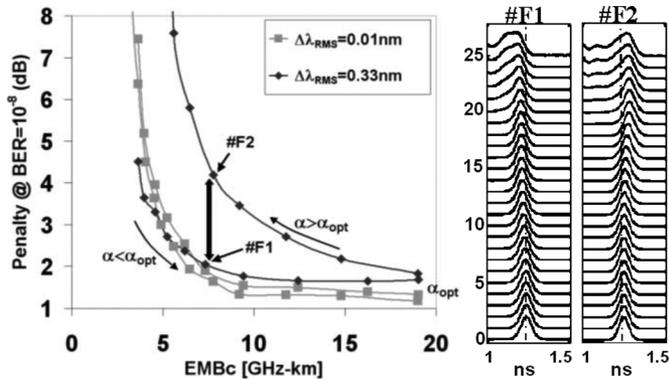
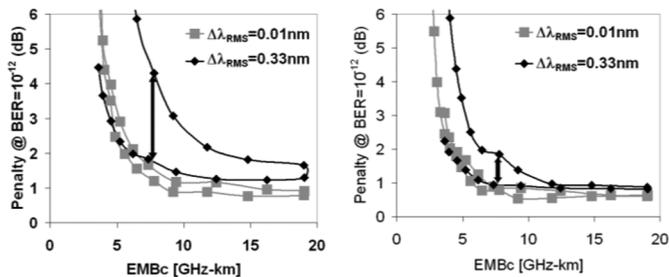Fig. 2. Correlation between EMBc and power penalty at a BER of 10^{-8} after 750 m.

Fig. 3. Correlation between EMBc and power penalty at a BER of 10^{-12} after 750 m (left) and 550 m (right).

Fig. 4. (a) Calculated radiation patterns of a three-transverse-mode VCSEL ($LP_{01}, LP_{11}, LP_{21}$); (b) spectrum of the VCSEL.

Fig. 5. (a) DMD plots of a fiber with $\alpha = \alpha_{\text{optimum}}$ at the three different λs; (b) "effective" DMD plots of the same fiber when used with a VCSEL with three modes at these $3\lambda s$.

B. Calculations

Fig. 2 shows the power penalty for a fixed BER $= 10^{-8}$ as a function of the EMBc of a 750-m-long MMF for which only the α parameter changes. The power penalty is the difference between the received powers for 750 and 2 m (back-to-back) transmissions for a fixed BER. The gray squares correspond to a single-mode VCSEL with a linewidth of 0.01 nm and the black diamonds correspond to a multimode VCSEL with a linewidth of 0.33 nm. These two VCSELs are chosen to provide the same encircled flux (EF) in the MMF.

For the single-mode VCSEL case, there is a good correlation between EMBc and system performance: MMFs with higher EMBc (lower modal dispersions) give lower power penalties. For the multimode VCSEL case, there is no correlation because of the effect of chromatic dispersion. MMFs with $\alpha < \alpha_{\text{optimum}}$ (e.g., fiber #F1) exhibit smaller power penalties than MMFs with $\alpha > \alpha_{\text{optimum}}$ (e.g., fiber #F2). Fibers have the same amounts of modal and chromatic dispersions but they interact with each other differently when the value of the α-parameter changes (MCDI effect). Note that this effect is also visible at a shorter distance of 550 m and at a smaller BER of 10^{-12} (see Fig. 3).

C. MCDI Effect

Transverse modes of VCSELs have different radiation patterns (higher order modes have most of their radiation power intensity far from the center [Fig. 4(a)] and they exhibit different wavelengths [Fig. 4(b)]. As a result, VCSEL spectra are spatially dependent.
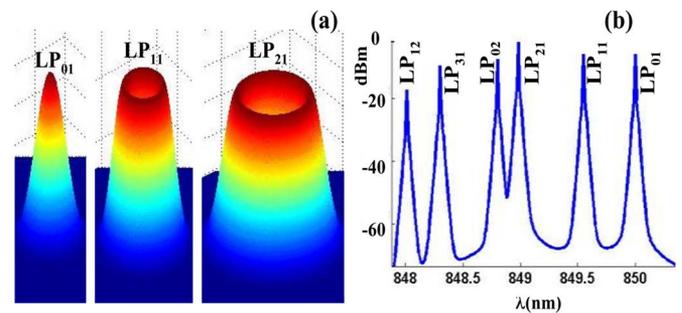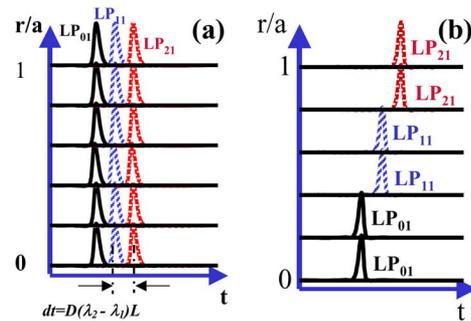
The consequence of these power and spectral characteristics is that the highest (respectively lowest) order modes of the VCSEL are mainly coupled into the highest (respectively lowest) order modes of the MMF, and that these highest (respectively lowest) order modes exhibit the smallest (respectively longest) wavelengths.

Independently of the modal dispersion, the highest order modes excited in the fiber exhibit an additional delay compared to the lowest order modes because of their lower wavelength and the effect of chromatic dispersion.

To better understand this effect, we consider the simple case of an MMF with no modal dispersion that only carries three guided modes. The DMD plots of such a fiber at three different wavelengths close to the operating wavelength are all straight [Fig. 5(a)]. However, the chromatic dispersion D introduces a delay between two DMD plots performed at different wavelengths λ_1 and λ_2. This delay is equal to $\Delta t = D(\lambda_2 - \lambda_1)L$, where L is the length of the fiber. As an example, at 850 nm, $D \sim -100$ ps/km $\cdot$ nm and $\lambda_1 - \lambda_2 = 1$ nm leads to $\Delta t = -100$ ps $\cdot$ km $= -0.1$ ps/m. This delay is of the order of magnitude of the maximum amount of modal dispersion allowed for a 10-GbE transmission over 550 m [7].

Now, if we consider that the highest (respectively lowest) order mode exhibits the smallest (respectively longest) wavelengths λ_1 (respectively λ_3), in accordance with the VCSEL characteristics, we obtain the "effective" DMD plots of
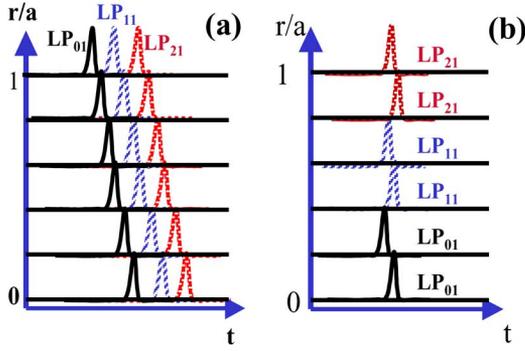
Fig. 6. (a) DMD plots of a fiber with $\alpha < \alpha_{\mathrm{optimum}}$ at the three different λs; (b) "effective" DMD plots: same fiber used with three-mode VCSEL at these $3\lambda s$.

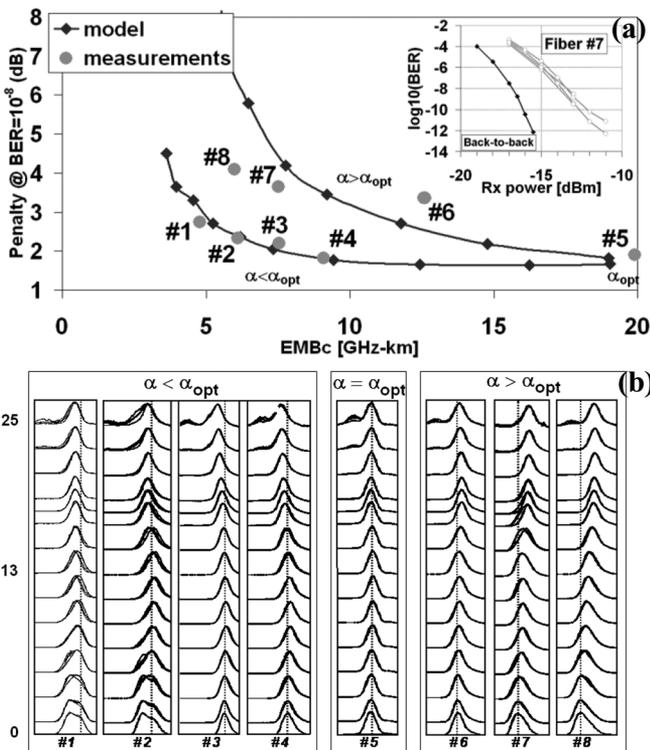
Fig. 7. (a) Power penalties at BER $= 10^{-8}$ for 750-m MMFs; (b) DMD plots of fibers.

Fig. 5(b), that are much closer to the fiber behavior when it is used with a VCSEL.

In this example of the perfect fiber exhibiting no modal dispersion, and thus with $\alpha = \alpha_{\mathrm{optimum}}$, we understand why the system performances will not be optimized.

An MMF with $\alpha < \alpha_{\mathrm{optimum}}$, for which the higher order modes travel faster than the lower order modes, appears to be more suited for VCSEL-based transmission systems (see Fig. 6). Indeed, in such a fiber, thanks to the spatial dependence of the spectrum of the VCSEL, the chromatic dispersion compensates for the modal dispersion of the fiber. This is in line with simulations of Figs. 2 and 3. Finally, MMFs with $\alpha > \alpha_{\mathrm{optimum}}$ will exhibit the poorest "effective" DMD plots.

III. Experimental Results

In order to experimentally assess this effect, we have performed power-penalty measurements at BER $= 10^{-8}$ in a 750-m-long 10-GbE system, using two commercially available VCSEL-based 10 GBASE-SR compliant transceivers: one at the emission side, providing a 0.33-nm rms spectral width, the other at reception side in order to avoid any crosstalk impairments [8].

Fig. 7(a) shows the calculated and measured power penalties at BER $= 10^{-8}$ as a function of EMBc. Fig. 7(b) shows the DMD plots of the MMFs used in the experiment. They mainly differ in α values with a center defect for some fibers. However, according to the EF, the influence of the center defect on the transmission is negligible. The MMFs 1 to 4 have $\alpha < \alpha_{\mathrm{optimum}}$ whereas MMFs 6 to 8 have $\alpha > \alpha_{\mathrm{optimum}}$.

As shown in Fig. 7(a), MMFs 1 to 4 exhibit lower penalties ($\sim$2 dB) than MMFs 6 to 8. The significant penalty difference between fibers 3 and 7, very close in EMBc, is a clear illustration of the MCDI effect. The MMF 5 with the best EMBc does not give the best system performance as predicted by the model.

Note that all the fibers have been extensively measured, for some down to a BER of 10^{-12}[8]. Their curves of sensitivities have not shown BER floors with the transmitter used in the experiment [see sensitivity of MMF 7 in inset of Fig. 7(a)], which is in agreement with our computations of Section II.

IV. Conclusion

We have theoretically and experimentally demonstrated that modal and chromatic dispersions interact with each other when MMFs are used with a transversally multimode VCSEL. It is possible, for a given VCSEL, to design an MMF for which the modal dispersion compensates for the chromatic dispersion, thus allowing better system performances. Because of this effect, when transmission distance increases, no clear correlation between EMBc and power penalty is observed.

References

[1] IEC 60793–1-49; Telecommunications Industry Association, TIA-455–220-A, Fiber Optic Test Procedures International Electrotechnical Committee, FOTP-220.

[2] P. Pepeljugoski, M. J. Hackert, J. S. Abbott, S. E. Swanson, S. E. Golowich, A. J. Ritger, P. Kolesar, Y. C. Chen, and P. Pleunis, "Development of system specification for laser-optimized 50 μm multimode fiber for multi-Gigabit short wavelength LANS," *J. Lightw. Technol.*, vol. 21, no. 5, pp. 1256–1275, May 2003.

[3] A. Gholami, D. Molin, P. Matthijsse, G. Kuyt, and P. Sillard, "A complete physical model for gigabit Ethernet optical communication systems," in *Proc. 57th Int. Wire and Cable Symp.*, 2008, pp. 289–294.

[4] A. Gholami, Z. Toffano, A. Destrez, S. Pellevrault, M. Pez, and F. Quentel, "Optimization of VCSEL spatiotemporal operation in MMF links for 10-Gigabit Ethernet," *IEEE J. Sel. Topics Quantum Electron.*, vol. 12, no. 4, pp. 767–775, Jul./Aug. 2006.

[5] P. Pepeljugoski, S. E. Golowich, A. J. Ritger, P. Kolesar, and A. Risteski, "Modeling and simulation of next-generation multimode fiber links," *J. Lightw. Technol.*, vol. 21, no. 5, pp. 1242–1255, May 2003.

[6] B. Stoltz and D. Yevick, "Calculated pulse responses of perturbed fiber profiles," *Appl. Opt.*, vol. 21, no. 23, pp. 4235–4240, 1982.

[7] *LAN/MAN CSMA/CD Access Method, Section 4*, IEEE Standard 802.3-2005.

[8] C. Caspar *et al.*, "Impact of transceiver characteristics on the performance of 10 GbE links applying OM-4 multimode fibers," in *Proc. 57th Int. Wire and Cable Symp.*, 2008, pp. 295–303.